

## Cleavage of amyloid precursor protein elicited by chronic cerebral hypoperfusion

S.A.L. Bennett<sup>a,\*</sup>, B.A. Pappas<sup>b</sup>, W.D. Stevens<sup>b</sup>, C.M. Davidson<sup>b,1</sup>, T. Fortin<sup>b</sup>, J. Chen<sup>a</sup>

<sup>a</sup>Department of Biochemistry, Microbiology, and Immunology, University of Ottawa, Ottawa, ON, Canada, K1H 8M5

<sup>b</sup>Institute of Neuroscience, Carleton University, 1125 Colonel By Drive, Ottawa, ON, Canada, K1S 5B6.

Received 14 October 1999; received in revised form 25 January 2000; accepted 29 February 2000

### Abstract

In the present study, we sought to determine whether low-grade, chronic vascular insufficiency induced in a rodent model of chronic cerebrohypoperfusion is sufficient, in and of itself, to trigger cleavage of the amyloid precursor protein (APP) into  $\beta$ A-sized fragments. We report that chronic two vessel occlusion (2VO) results in progressive accumulation of  $\beta$ A peptides detected by Western analysis in aged rats correlating with a shift in the immunohistochemical localization of APP from neurons to extracellular deposits in brain parenchyma. These data indicate that the 2VO paradigm reproduces features of  $\beta$ A biogenesis characteristic of sporadic Alzheimer's disease. © 2000 Elsevier Science Inc. All rights reserved.

**Keywords:** Amyloid precursor protein;  $\beta$ -amyloid; Chronic vascular insufficiency; Alzheimer's disease; Chronic ischemia

### 1. Introduction

It is well established that the integrity of the cerebral vasculature is essential to maintaining cognitive function during aging (for a review see [8]). Chronic disruption of cerebral blood flow resulting from carotid insufficiency and other ischemic states associated with aging can induce neurological deficits and dementia [2,7,17,18]. These conditions are exacerbated during arteriosclerosis-induced dementia and Alzheimer's disease by cerebral angiopathy and morphological aberrations in brain microvasculature [11]. Although circulation-dependent behavioral deficits can be modelled in experimental paradigms of chronic cerebrovascular insufficiency, the impact of protracted low-grade blood flow reduction on amyloid precursor protein (APP) metabolism in the absence of other disease factors is still ambiguous [5,6,15,18].

In Alzheimer's disease, membrane-bound APP is proteolytically processed into  $\beta$ A-sized fragments (8–15kDa) by the sequential actions of  $\beta$ - and  $\gamma$ -secretases. These aberrant

fragments can accumulate both intraneuronally and as extracellular deposits in brain parenchyma, exerting cytotoxic effects on neurons and increasing vascular permeability [13,21,23,24]. The cerebrovascular actions of  $\beta$ A peptides render transgenic animals overexpressing APP more susceptible to ischemic injury presumably by increasing vascular reactivity thereby eliciting more severe ischemia in infarcted regions [24]. Conversely, ischemic attack has also been implicated in the etiology of  $\beta$ A deposition. After transient ischemic attack, post-translational modification of APP into  $\beta$ A-sized fragments and subsequent extracellular  $\beta$ A deposition in brain parenchyma have been observed in ischemic tissue [1,12,20,22]. The increase in APP, however, may not always lead to neuropathological  $\beta$ A-associated cleavage. After 3–4 weeks of bilateral carotid artery occlusion, hippocampal APP immunoreactivity is only marginally increased [10]. Cleavage of the parent protein to  $\beta$ A-sized fragments after chronic ischemia was not addressed in this study [10]. In experimental models of repeated ischemic attacks, APP protein expression and  $\beta$ A accumulation have been demonstrated not only in damaged tissue but also in regions spared ischemic insult, thereby implicating APP synthesis in both neuropathology and neural protection [9,10]. The only report, to our knowledge, of APP processing in a chronic model of ischemia has demonstrated enhanced APP cleavage in animals treated prophylactically

\* Corresponding author. Tel.: +1-613-562-5800; fax: +1-613-562-5440.

E-mail address: sbennet@aix1.uottawa.ca (S.A.L. Bennett).

<sup>1</sup> Current address: Department of Pathology, Queens University, Kingston, ON, Canada

with propentofylline (and thus spared severe ischemic injury) relative to untreated ischemic animals [16]. Thus, it is unclear whether changes in APP post-translation modification after cerebral ischemia are, in fact, neuroprotective or whether they contribute to progressive neurodegeneration elicited by chronic cerebral hypoperfusion. Furthermore, it is unknown whether chronic low-grade cerebral ischemia leads to  $\beta$ A-deposition or whether  $\beta$ A-associated cleavage is only elicited by severe ischemia/reperfusion injury.

In the present study, we sought to characterize APP processing in an experimental model of sustained low-grade ischemia. In rodents, permanent ligation of the common carotid arteries (2VO) induces morphological abnormalities in neurons and quantifiable cell loss within 7 months of blood flow reduction [5,15,18]. Using the 2VO paradigm, we have demonstrated that a moderate but chronic reduction of cerebral blood flow elicits protracted gliosis, incremental apoptotic death in neurons in rat hippocampus, and progressive behavioral impairment [3,4,15]. We now report that the low grade chronic vascular insufficiency induced by 2VO is, in and of itself, sufficient to trigger cleavage of APP into  $\beta$ A-sized fragments and induce extracellular accumulation of APP proteolytic products.

## 2. Materials and methods

### 2.1. Induction of chronic cerebral hypoperfusion by two vessel occlusion (2VO) surgery

Permanent bilateral carotid occlusion resulting in sustained low-grade ischemia was induced in male Sprague Dawley retired breeders (Charles River Laboratories, PQ), approximately 10 months of age ( $n = 20$ ), as described in [3,15]. Sham surgeries were performed on age-matched control rats ( $n = 17$ ). Rats were anesthetized with ketamine hydrochloride (100 mg/kg IM) and sodium methohexital (40 mg/kg IP). A ventral midline incision was made to expose the carotid arteries and the blood vessels were gently isolated from the carotid sheath and vagus nerve. In 2VO surgery, each carotid artery was double-ligated with 5–0 silk suture just below the vascular bifurcation. In sham operations, arteries were exposed but not ligated. Rats were closely monitored during postoperative recovery and body temperature maintained with a servo-controlled heating pad. Animals were sacrificed at 2 ( $n = 3$  2VO;  $n = 2$  sham), 10 ( $n = 4$  2VO;  $n = 3$  sham), 20–27 ( $n = 5$  2VO;  $n = 5$  sham), and 40 ( $n = 8$  2VO;  $n = 7$  sham) weeks after surgery.

For Western analyses, rats sacrificed at 2, 10, and 20–27 weeks were deeply anesthetized with sodium pentobarbital and euthanized by decapitation. Brains were rapidly removed and blocked coronally at approximately bregma  $-1.8$  and bregma  $-6.04$ . The dorsal and ventral hippocampi were removed. Cortices and remaining medial structures were blocked horizontally at the rhinal fissure. The dorsolateral cortex encompassing the somatosensory,

parietal, and cingulate cortices was separated from thalamus and corpus callosum. The ventrolateral cortex encompassing the entorhinal and piriform cortices and amygdaloid nuclei was separated from optic tract, hypothalamus, and ventral thalamic nuclei. Hippocampal and cortical protein was isolated using Triazol (Life Sciences Research Technologies, Mississauga, ON, Canada) according to the protocol provided by the manufacturer. For  $n = 5$  animals/condition sacrificed at 20–27 weeks post surgery, protein extracts were prepared separately from each animal for hippocampus and combined dorsolateral and ventrolateral cortices. For all other animals, tissue was pooled at each time point prior to protein extraction.

For immunohistochemical analysis, animals sacrificed at 40 weeks postsurgery ( $n = 5$  per condition) were deeply anesthetized with sodium pentobarbital and euthanized by cardiac perfusion with heparinized saline followed by 4% paraformaldehyde in 100 mM phosphate buffer (pH 7.4). Brains were postfixed in phosphate-buffered 4% paraformaldehyde for 24 h at 4°C and tissue was paraffin-embedded according to standard histological procedure. Coronal sections were cut on a rotary microtome at 8  $\mu$ m. Sections at approximately bregma  $-3.8$  were analyzed. All manipulations were performed in compliance with approved institutional protocols and according to the strict ethical guidelines for animal experimentation established by the Medical Research Council (Canada).

### 2.2. Western analyses

Protein (40  $\mu$ g) was separated by SDS-PAGE under reducing conditions on 12.5% and 7.5% polyacrylamide gels containing 0.1% (w/v) SDS and electroblotted to Immobilon membrane. Membranes were incubated overnight with either polyclonal antibody anti- $\beta$ A (1:5, Roche, Laval, PQ) or monoclonal antibody anti-APP (1:10; Roche). Anti- $\beta$ A was raised against the synthetic peptide DAEFRH-DSGYEVHHQKLLVFFAEDVGSNKGAIIGLMVGGVIA recognizing C-terminal epitopes located between amino acids 597–638 of human APP. Anti- $\beta$ A detects amyloidogenic  $\beta$ A in both human and rat. Anti-APP was raised against the final C-terminus amino acids 642–695 of human APP and detects APP, intermediate-sized fragments, and short carboxyl fragments released during final amyloidogenic  $\beta$ A processing in both human and rat. Secondary antibodies were a horse radish peroxidase-conjugated anti-rabbit IgG (1:400; Roche) or a horseradish peroxidase-conjugated anti-mouse IgG (1:1000; Jackson Immunolabs, West Grove, PA, USA). Immunoreactive fragments were visualized by chemiluminescence according to the protocol established by the manufacturer (Pierce, Rockford, IL, USA). In control reactions, membranes were incubated with secondary reagent in the absence of primary antibody. In all reactions, membranes were blocked in 10 mM PBS (10 mM sodium phosphate buffer, pH 7.5, 154 mM NaCl) containing 1% heat-denatured casein and washed repeatedly between reac-

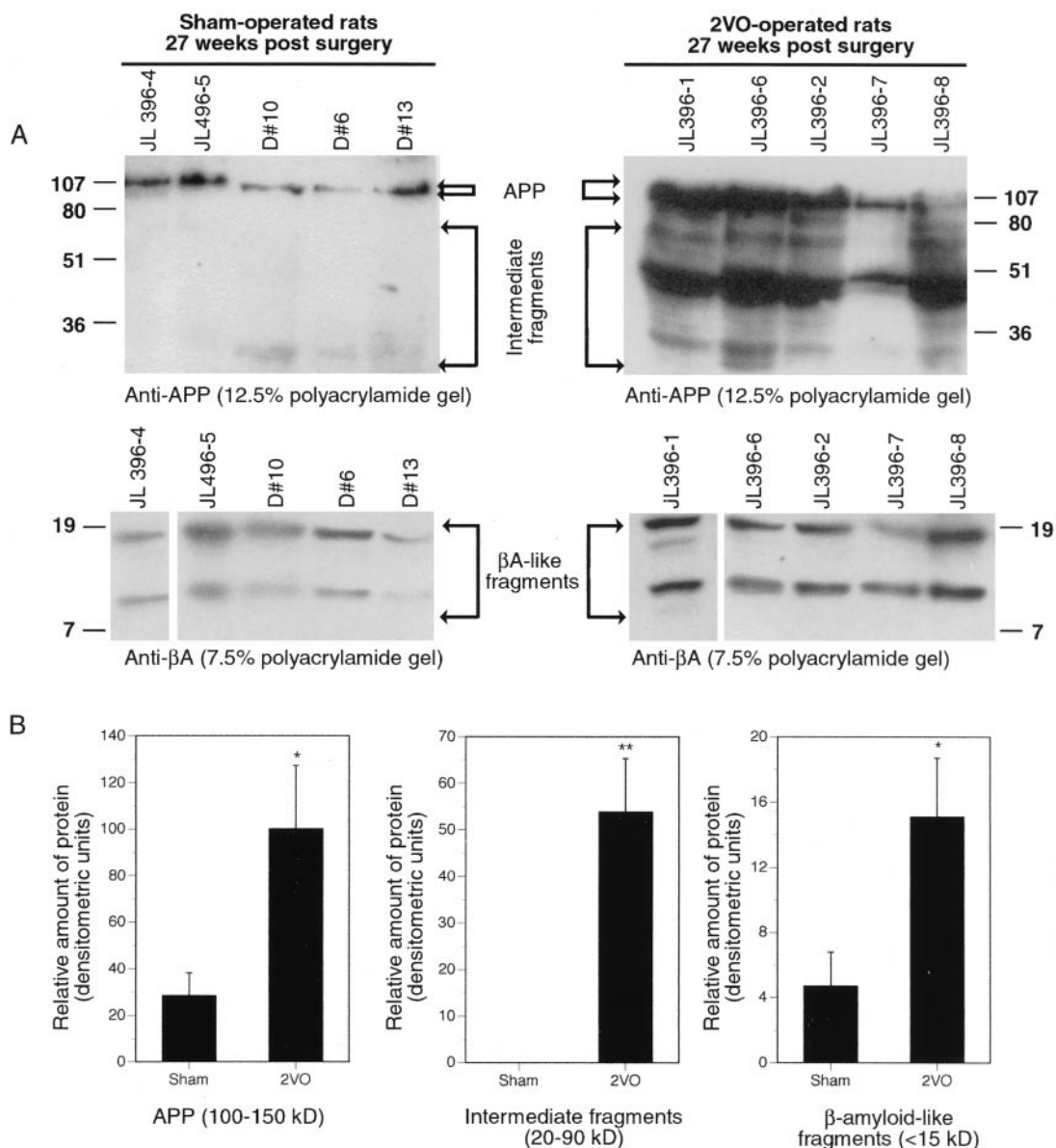


Fig. 1. Increased APP protein expression and APP cleavage into intermediate- and  $\beta$ A-sized fragments are detected in rat parietal-temporal cortex 20–27 weeks after 2VO surgery. Protein (40  $\mu$ g) was subjected to Western analysis using anti-APP to detect APP and intermediate cleavage fragments (A, upper blots) or anti- $\beta$ A to detect  $\beta$ A-sized fragments (A, lower blots) as described in Materials and methods. Blots were reacted with antibodies simultaneously and exposed for identical periods of time. Densitometry was performed on exposures that fell within linear range for analysis as described in Materials and methods. Figures depict longer exposure times than those used for densitometry. A significant increase in the amounts of APP detected and in the production of  $\beta$ A-sized fragments was detected in 2VO-operated rats relative to sham-operated rats (Panel B). A significant increase in the cleavage of intermediate sized fragments was detected in 2VO-operated rats relative to sham-operated rats (Panel B). \* $P < 0.05$ . \*\* $P < 0.01$ .

tions in blocking solution containing 0.35% Tween-20 (anti- $\beta$ A) or 0.1% Tween-20 (anti-APP). Antibodies were diluted in blocking solution lacking Tween-20.

Densitometry was performed on a LKB Ultrascan Enhanced Laser Densitometer running GelScan XL software (Pharmacia, Baie d'Urfé, PQ). Data are presented as relative amount of protein as defined by the "Area(%)" value (the relative to total integrated area of the absorbance peak) multiplied by 100. The "Area(%)" $\times$ 100 value is expressed as densitometric units. Values under 200 fall within in linear range for densitometric analysis. To obtain Western blots

within linear range, multiple exposures were developed. Statistical analysis were only performed on blots for which maximal signal intensity was below 200. Only blots that were developed simultaneously were compared statistically. Densitometric data were analyzed by Student's *t* test comparing 2VO versus sham with  $\alpha$  set at  $P < 0.05$ .

### 2.3. Immunohistochemistry

Paraffin-embedded sections were deparaffinized in clearane, rehydrated through a series of graded alcohols,

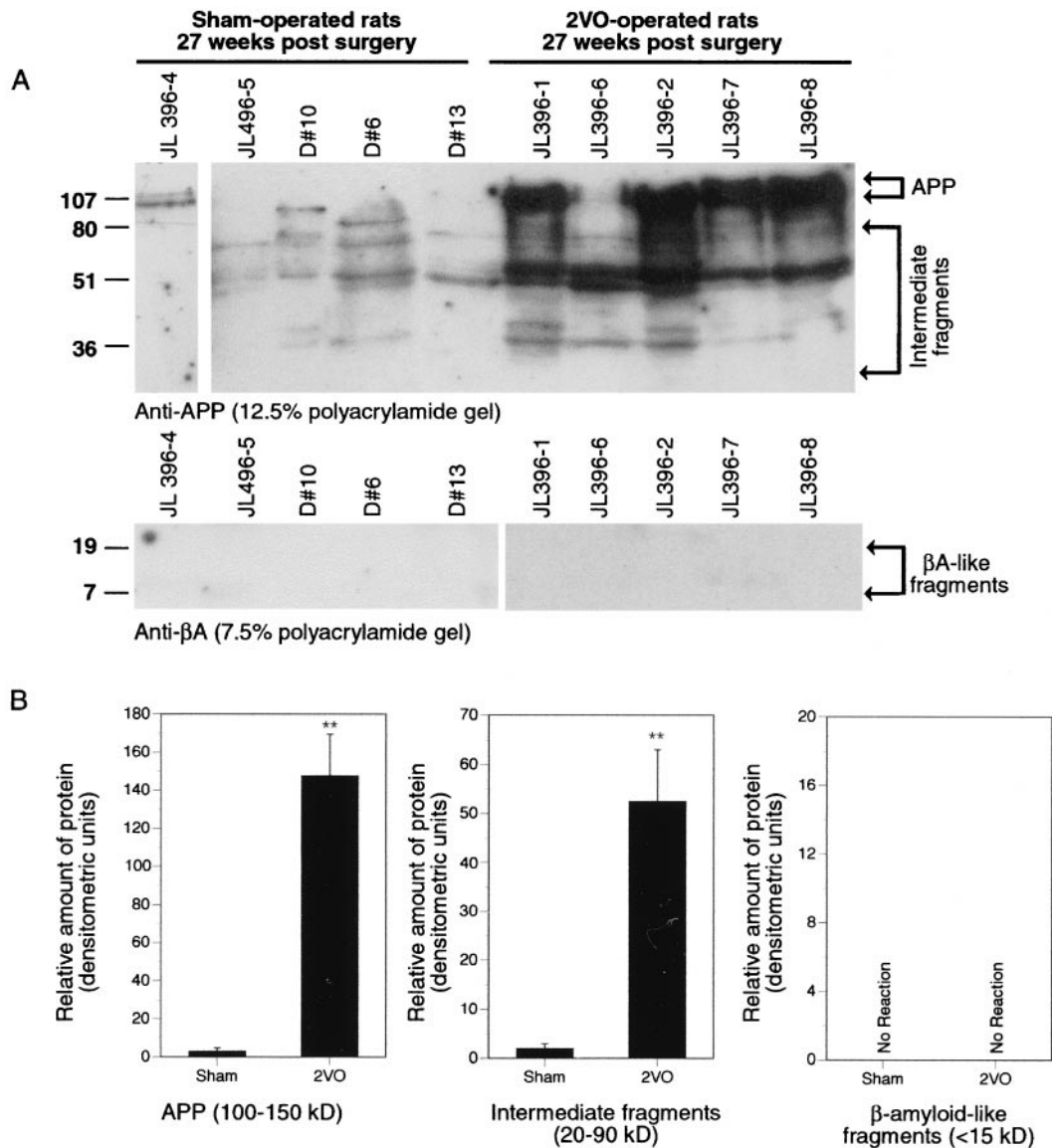


Fig. 2. Increased APP protein expression and APP cleavage into intermediate-sized fragments but not  $\beta$ A is detected in rat hippocampus after 2VO surgery. Protein (40  $\mu$ g) was subjected to Western analysis using anti-APP to detect APP and intermediate cleavage fragments (A, top) or anti- $\beta$ A to detect  $\beta$ A-sized fragments (A, bottom) as described in Section 2. Blots were reacted with antibodies simultaneously and exposed for identical periods of time. Densitometry was performed on exposures that fell within linear range for analysis as described in Materials and methods. Figures depict longer exposure times than those used for densitometry. A highly statistically significant increase in the amounts of APP detected and in the cleavage of intermediate sized fragments was detected in 2VO-operated rats relative to sham-operated rats (B).  $\beta$ A-sized fragments were not detected in either condition.

and equilibrated in 10 mM PBS (10 mM sodium phosphate buffer, pH 7.2, 154 mM NaCl). Sections were reacted overnight with primary antibody (APP, 1:100) at 4°C, labeled for 1 h at room temperature with biotinylated goat anti-mouse IgG (1:300; Sigma Chemical Co., St. Louis, MO, USA), incubated for 1 h in extravidin-peroxidase (1:40, Sigma), and reacted with 1 mg/ml diaminobenzidine in 50 mM Tris-HCl, pH 8.0 containing 0.003% H<sub>2</sub>O<sub>2</sub>. Antibodies and tertiary reagents were diluted in Ab buffer (10 mM PBS, 0.3% Triton-X, 3% BSA, pH 7.2).

### 3. Results

#### 3.1. Changes in APP processing elicited by 2VO

Retired male Sprague Dawley breeders were 10 months old at the time of sham ( $n = 5$ ) or 2VO surgery ( $n = 5$ ). Rats were sacrificed between 20 and 27 weeks after surgery. Brains were blocked coronally at approximately bregma  $-1.8$  and bregma  $-6.04$ . Western immunoblots of protein extracts from the parietal-temporal cortex and the hippocampal formation were analyzed. In

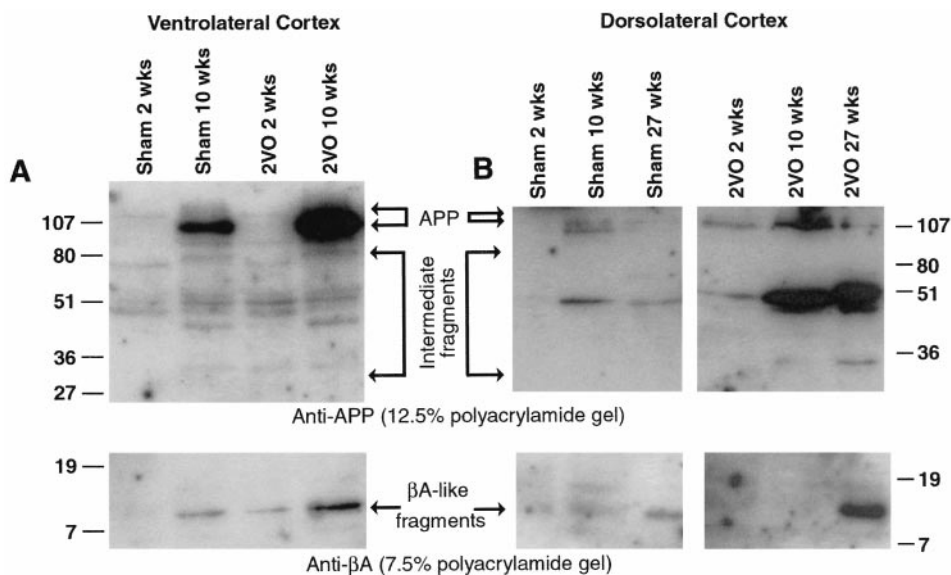


Fig. 3. A time-dependent increase in APP cleavage is detected in rat ventrolateral and dorsolateral cortex following 2VO surgery. Protein was isolated from rat ventrolateral (A) and dorsolateral (B) cortices. Protein was pooled from tissue extracted from 2-week 2VO animals ( $n = 3$ ), 2-week sham animals ( $n = 2$ ), 10-week 2VO animals ( $n = 4$ ), 10-week sham animals ( $n = 3$ ), 27-week 2VO animals ( $n = 3$ , dorsolateral cortex only), and 27-week sham animals ( $n = 2$ , dorsolateral cortex only). Western analysis was performed using anti-APP (upper blots) to detect APP and intermediate cleavage fragments or anti- $\beta$ A (lower blots) to detect  $\beta$ A-sized fragments as described in Materials and methods.

parietal-temporal cortex, a significant increase in the amounts of APP proprotein ( $t = 2.49$ ,  $df = 8$ ,  $P < 0.05$ ), intermediate sized degradative products ( $t = 4.72$ ,  $df = 8$ ,  $P < 0.01$ ), and  $\beta$ A-like fragments ( $t = 2.51$ ,  $df = 8$ ,  $P < 0.05$ ) were observed in 2VO-operated rats relative to sham-operated rats (Fig. 1A and B). In the hippocampus, a significant increase in the amounts of APP proprotein ( $t = 6.58$ ,  $df = 8$ ,  $P < 0.01$ ) and intermediate-sized degradative products ( $t = 4.73$ ,  $df = 8$ ,  $P < 0.01$ ) were observed in 2VO- compared to sham-operated rats (Fig. 2A and B). Cleavage of APP into  $\beta$ A-sized fragments was not detected in rat hippocampus 20–27 weeks after 2VO surgery.

To qualitatively examine the kinetics of this cleavage, replicate Western blots were performed on pooled protein samples extracted from animals sacrificed at 2 ( $n = 3$  2VO;  $n = 2$  sham), 10 ( $n = 4$  2VO;  $n = 3$  sham), or 27 ( $n = 3$  2VO;  $n = 2$  sham) weeks after surgery. Densitometry was not performed, given that protein samples were pooled across subjects and immunoblots were only conducted in replicate. To more precisely isolate changes in parietal-temporal cortex, tissue was dissected into dorsolateral cortex encompassing the somatosensory, parietal, and cingulate cortices and ventrolateral cortex encompassing the entorhinal and piriform cortices and amygdaloid nuclei prior to extraction. In ventrolateral cortex of sham-operated rats, bands corresponding to full-length APP, proteolytic intermediate products, and potentially amyloidgenic  $\beta$ A were identified (Fig. 3A). An increase in APP proprotein levels was consistently observed over time after both sham and 2VO surgery with a more pronounced increase noted in

2VO rats (Fig. 3A, top; compare 2- and 10-week lanes in both sham and 2VO conditions).  $\beta$ A cleavage was detected at 10 weeks postsurgery in sham-operated animals, but not at earlier time-points (Fig. 3A, bottom; compare sham 2 and 10 week lanes). Synthesis of this potentially amyloidgenic isoform was accelerated by 2VO surgery. Animals exhibited a 12kDa anti- $\beta$ A immunoreactive band 2 weeks after 2VO surgery but not sham surgery, with a marked increase in synthesis observed at 10 weeks (Fig. 3A, bottom; compare 2VO 2- versus 10-week lanes). In dorsolateral cortex, full-length APP, intermediate proteolytic products, and  $\beta$ A sized fragments were detected (Fig. 3B). Maximal levels of APP proprotein were observed 10 weeks after sham or 2VO surgery (Fig. 3B, top). Consistent with data presented for  $n = 5$  animals in Fig. 1, 2VO rats synthesized more APP and intermediate sized fragments than sham-operated animals 27 week after surgery (Fig. 3B, top; compare sham and 2VO 27 week lanes). Although a progressive accumulation of  $\beta$ A fragments was observed between 2 and 27 weeks postsurgery in sham-operated animals, this increase was markedly augmented following 2VO surgery (Fig. 3B, bottom).

In hippocampus, full length APP isoforms were detected in sham-operated animals with an increase in synthesis over time after surgery (Fig. 4A; compare sham 2- and 10-week lanes). 2VO surgery was associated with an even greater increase in the levels of intermediate proteolytic fragments (Fig. 4A; compare sham and 2VO lanes). As with later time points (Fig. 2),  $\beta$ A proteolytic products were not detected in hippocampus following sham or 2VO surgery (Fig. 4B).

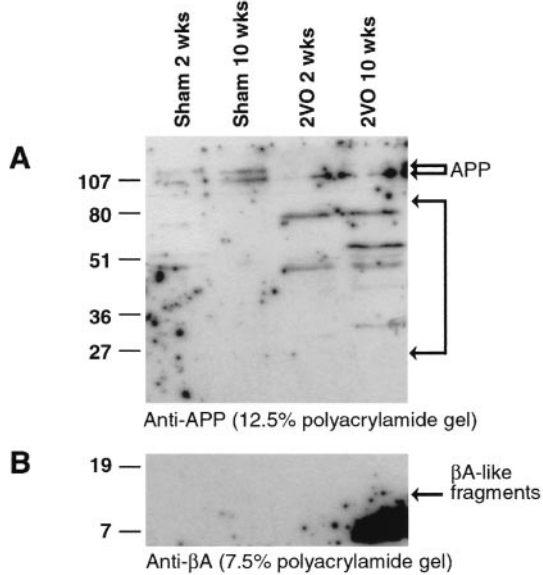


Fig. 4. APP cleavage into intermediate proteolytic fragments increases over time in rat hippocampus following 2VO surgery. Protein was isolated from 2-week 2VO animals ( $n = 3$ ), 2-week sham animals ( $n = 2$ ), 10-week 2VO animals ( $n = 4$ ), or 10-week sham animals ( $n = 3$ ). Western analysis was performed using anti-APP to detect APP and intermediate cleavage fragments (A) or anti- $\beta$ A to detect  $\beta$ A-sized fragments (B) as described in Section 2.

### 3.2. Extracellular deposition of APP biosynthetic products

Immunohistochemistry for APP was performed using anti-APP at 40 weeks post 2VO or sham surgery. Consistent with the reduction in full length APP synthesis observed by Western analysis after 20–27 weeks of 2VO, a qualitative decrease in the extent of neuronal reactivity was observed 40 weeks after surgery in 2VO rats (Fig. 5B) compared to sham-operated animals (Fig. 5A). Notably, de novo extracellular deposition of APP immunoreactive deposits was evident in brain parenchyma of 2VO animals in ventrolateral cortex (Fig. 5B); an area that exhibited APP cleavage consistent with production of  $\beta$ A by Western analysis. Depositions were not observed in areas that failed to exhibit  $\beta$ A biosynthesis (i.e. hippocampus; data not shown).

### 4. Conclusions

In the present study, we characterize APP cleavage in aging rodent hippocampus and parietal-temporal cortex after induction of low-grade chronic vascular insufficiency. Our results indicate that chronic cerebrohypoperfusion elicited by 2VO is sufficient to stimulate aberrant APP process-

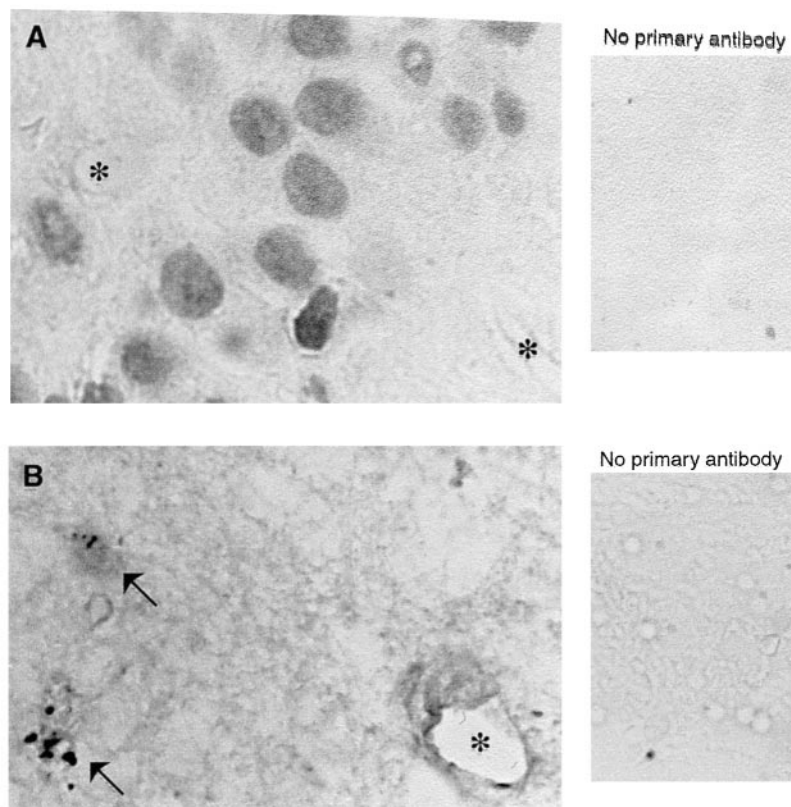


Fig. 5. Immunohistochemical localization of APP in ventrolateral cortex of sham- and 2VO-operated rats 40 weeks after surgery. Immunohistochemistry was performed using anti-APP as described in Materials and methods. (A) Sham-operated ventrolateral cortex. Note neuron-associated labeling of APP. (B) 2VO-operated ventrolateral cortex. Note the reduction of APP immunoreactivity in neurons and extracellular deposition of material in brain parenchyma (B). Anti-APP immunoreactive extracellular deposits were not detected in brain regions that failed to exhibit  $\beta$ A-sized fragments by Western analysis (i.e., hippocampus). Right-hand panel depicts staining of adjacent sections in the absence of primary antibody.

ing including production of potentially amyloidogenic  $\beta$ A and accumulation of extracellular  $\beta$ A deposits in rat cortex in the absence of any other disease factors. These data suggest that chronic cerebral hypoperfusion may contribute to the alterations in APP biosynthesis associated with Alzheimer's disease.

#### 4.1. Biogenesis of $\beta$ A-elicited by 2VO

APP proteolysis to  $\beta$ A-sized fragments was observed in rodents after 2VO in parietal-temporal cortex but not hippocampus. In cortical tissue, full-length partially glycosylated APP (100 kDa), intermediate proteolytic fragments (20–90 kDa), and smaller  $\beta$ A-like products (<15 kDa) were detected by Western analysis.  $\beta$ A biogenesis was observed at low levels in sham-operated rats in these brain regions. However, accumulation of  $\beta$ A-sized fragments was exacerbated over time in cortical tissue after 2VO with synthesis more pronounced in ventrolateral parietal-temporal cortex. This sustained accumulation of  $\beta$ A associated with 2VO surgery correlated with a subsequent shift in immunohistochemical localization of APP from neuron-associated staining to extracellular deposits in brain parenchyma.  $\beta$ A-associated cleavage was not detected in hippocampus, although an increase in intermediate proteolytic APP fragments was noted over time after 2VO-surgery. To our knowledge, this finding represents the first time that aberrant APP processing characteristic of normal aging and late-onset Alzheimer's disease has been demonstrated in a rodent model of low grade chronic vascular insufficiency in the absence of any other disease factors.

#### 4.2. Comparison with APP processing in Alzheimer's brain

The primary difference between APP processing observed in the 2VO rodent model of chronic vascular insufficiency and APP proteolysis detected in Alzheimer's tissue is the regional localization of proteolytic events. In Alzheimer's brain,  $\beta$ A-associated cleavage is frequently detected in both hippocampus and parietal-temporal cortex. The lack of  $\beta$ A accumulation in rodent hippocampus may be the result of regional differences in cerebral hypoperfusion elicited. Previous work has demonstrated that the chronic reductions in blood flow after 2VO are more pronounced in cortical structures than in hippocampus. 2VO in rat elicits sustained low-grade ischemia characterized by an immediate 50% reduction in cerebral blood flow to hippocampal and a 75% reduction in cerebral blood flow to cortical structures within hours of 2VO surgery [14,19]. A chronic 25% reduction in cerebral blood flow to hippocampal and a 40% reduction in cerebral blood flow to cortical structure is observed within days of carotid ligation [14,19]. No further improvements in cerebral blood flow are detected after several months of 2VO [5,14,19]. Thus, it is consistent that  $\beta$ A-associated proteolytic events elicited by sustained hy-

poperfusion would be more pronounced in cortical than hippocampal structures.

## 5. Conclusion

In the present study, we sought to characterize APP processing in an experimental model of sustained low-grade ischemia. We have previously demonstrated that a moderate but chronic reduction of cerebral blood flow elicits neuropathology associated with progressive behavioral impairment. We now demonstrate that 2VO can trigger  $\beta$ A biogenesis and deposition of extracellular amyloid deposits in the absence of any other disease factors. These data demonstrate that chronic low grade cerebral hypoperfusion has effects on APP proteolytic processing similar to those associated with sporadic Alzheimer's disease and suggests that chronic 2VO will be a useful model to investigate the behavioral effects of aberrant APP cleavage.

## Acknowledgments

This work was funded by grants from the Ontario Mental Health Foundation (Canada) and Scottish Rite Charitable Foundation (Canada) to S.A.L.B. and the Ontario Heart and Stroke Foundation to B.A.P. We thank J. Bennett for critical and technical assistance.

## References

- [1] Baiden–Amisshah K, Joashi U, Blumberg R, Mehmet H, Edwards AD, Cox, PM. Expression of amyloid precursor protein (beta-APP) in the neonatal brain following hypoxic ischemic injury. *Neuropathol Appl Neurobiol* 1998;24:346–52.
- [2] Barrow DL. Unruptured cerebral arteriovenous malformations presenting with intracranial hypertension. *Neurosurgery* 1988;23:484–90.
- [3] Bennett SAL, Tenniswood M, Chen J-H, et al. Chronic cerebral hypoperfusion elicits neuronal apoptosis and behavioral impairment. *Neuroreport* 1998;9:161–6.
- [4] Davidson CM, Pappas BA, Stevens WD, Fortin T, Bennett SAL. Chronic cerebrohypoperfusion: loss of pupillary reflex, visual impairment, and retinal neurodegeneration. *Brain Res* 2000;859:96–103.
- [5] de la Torre JC, Fortin T, Park, GAS.; Pappas, BA., Richard, MT.. Brain blood flow restoration 'rescues' chronically damaged rat CA1 neurons. *Brain Res* 1993;623:6–15.
- [6] de la Torre JC, Fortin T, Park GAS, et al. Chronic cerebrovascular insufficiency induces dementia-like deficits in aged rats. *Brain Res* 1992;582:186–95.
- [7] de la Torre JC, Mussivand T. Can disturbed brain microcirculation cause Alzheimer's disease? *Neurol Res* 1993;15:146–53.
- [8] Kalaria RN. Cerebral vessels in ageing and Alzheimer's Disease. *Pharmacol Ther* 1996;72:193–214.
- [9] Kalaria RN, Bhatti SU, Lust WD, Perry G. The amyloid precursor protein in ischemic brain injury and chronic hypoperfusion. *Ann NY Acad Sci* 1993;695:190–3.
- [10] Kalaria RN, Bhatti SU, Palatinsky EA, et al. Accumulation of beta-amyloid at sites of ischemic injury in rat brain. *Neuroreport* 1993;4:211–4.

- [11] Kalaria RN, Hedera P. Differential degeneration of the cerebral microvasculature in Alzheimer's disease. *Neuroreport* 1995;6:477–80.
- [12] Lin B, Schmidt-Kastner R, Busto R, Ginsberg, MD. Progressive parenchymal deposition of beta-amyloid protein in rat brain following global cerebral ischemia. *Acta Neuropathol* 1999;97:359–68.
- [13] Nishimura L, Uetsuki T, Dani SU, et al. Degeneration *in vivo* of rat hippocampal neurons by wild-type Alzheimer amyloid precursor protein overexpressed by adenovirus-mediated gene transfer. *J Neurosci* 1998;18:2387–98.
- [14] Otori T, Katsumata T, Katayama Y, Terashi A. Measurement of regional cerebral blood flow and glucose utilization in rat brain under chronic hypoperfusion conditions following bilateral carotid artery occlusion. Analyzed by autoradiographical methods. *Nippon Ika Daigaku Zasshi* 1997;64:428–39.
- [15] Pappas BA, de la Torre JC, Davidson CM, Keyes MT, Fortin T. Chronic reduction of cerebral blood flow in the adult rat: late-emerging CA1 cell loss and memory dysfunction. *Brain Res* 1996;708:50–8.
- [16] Plaschke K, Martin E, Bardenheuer HJ. Effect of propentofylline on hippocampal brain energy state and amyloid precursor protein concentration in a rat model of cerebral hypoperfusion. *J Neural Transm* 1998;105:1065–77.
- [17] Schmidt-Kastner R, Fliss H, Hakim, AH. Subtle neuronal death in striatum after short forebrain ischemia in rats detected by *in situ* end-labeling for DNA damage. *Stroke* 1997;28:163–70.
- [18] Sekhon LHS, Morgan MK, Spence I, Weber N. Chronic cerebral hypoperfusion: pathological and behavioral consequences. *Neurosurgery* 1997;40:548–56.
- [19] Tsuchiya M, Sako K, Yura S, Yonemasu Y. Cerebral blood flow and histopathological changes following bilateral carotid artery ligation in Wistar rats. *Exp Brain Res* 1992;89:87–92.
- [20] Uehara H, Yoshioka H, Kawase S, et al. A new model of white matter injury in neonatal rats with bilateral carotid artery occlusion. *Brain Res* 1999;837:213–20.
- [21] Uetsuki T, Takemoto K, Nishimura I, et al. Activation of neuronal caspase-3 by intracellular accumulation of wild-type Alzheimer amyloid precursor protein. *J Neurosci* 1999;19:6955–64.
- [22] Yokaota M, Saido TC, Tani E, Yamaura I, Minami N. Cytotoxic fragment of amyloid precursor protein accumulates in hippocampus after global forebrain ischemia. *Cereb Blood Flow Metab* 1996;16:1219–23.
- [23] Yoshikawa K, Aizawa T, Hayashi Y. Degeneration *in vitro* of post-mitotic neurons overexpressing the Alzheimer amyloid protein precursor. *Nature* 1992;359:64–7.
- [24] Zhang F, Eckman C, Younkin S, Hsiao KK, Iadecola C. Increased susceptibility to ischemic brain damage in transgenic mice overexpressing the amyloid precursor protein. *J Neurosci* 1997;17:7655–61.